NUCLEAR SCIENCE AND TECHNIQUES **26**, S10301 (2015)

# Adsorption behavior of $^{241}$Am(III) and Eu(III) by silica/polymer-based *iso*Hex-BTP adsorbent from nitric acid solution*

LIU Rui-Qin (刘瑞芹),[1] WANG Xin-Peng (王欣鹏),[1] NING Shun-Yan (宁顺艳),[1] WEI Yue-Zhou (韦悦周),[1,†]
YANG Jin-Ling (杨金玲),[2] ZHAO Ya-Ping (赵雅平),[2] and DING You-Qian (丁有钱)[2]

[1] *School of Nuclear Science and Engineering, Shanghai Jiao Tong University, 800 Dongchuan Road, Shanghai 200240, China*
[2] *China Institute of Atomic Energy, Beijing 102413, China*

(Received May 6, 2014; accepted in revised form July 19, 2014; published online December 20, 2014)

The adsorption behavior of $^{241}$Am(III) and Eu(III) by silica/polymer-based *iso*Hex-BTP adsorbent (*iso*Hex-BTP/$SiO_2$-P) was investigated by a batch experiment method. *iso*Hex-BTP/$SiO_2$-P exhibited high affinity and selectivity for $^{241}$Am(III) over $^{152}$Eu(III) in 2–4 mol/dm$^3$ nitric acid solutions. Within the experimental contact time range of 0.5–24 h, *iso*Hex-BTP/$SiO_2$-P showed high selectivity for $^{241}$Am(III) compared to $^{152}$Eu(III) in 3 mol/dm$^3$ nitric acid solution. However, the adsorption kinetics of $^{241}$Am(III) and $^{152}$Eu(III) was slow. Eu(III) adsorption followed the pseudo-second-order kinetic model, indicating chemical adsorption as the rate-limiting step of the adsorption process. And the adsorption agreed well with the Langmuir adsorption model at various temperatures. The adsorption kinetics and isotherm data indicated that the equilibrium adsorption capacity, the adsorption rate, the maximum adsorption capacity and the adsorption affinity, increased with temperature. The thermodynamic parameters, negative change in Gibbs free energy, and positive change in enthalpy and entropy, suggested that the adsorption of Eu(III) was spontaneous and endothermic process with an increase of entropy.

Keywords: *iso*Hex-BTP/$SiO_2$-P, Extraction chromatography, High level liquid waste (HLLW), Am(III), Eu(III)

DOI: 10.13538/j.1001-8042/nst.26.S10301



## I. INTRODUCTION

The selective partitioning of trivalent minor actinides (MA(III): Am(III) and Cm(III)) from the bulk of trivalent lanthanides (Ln(III)) present in high level liquid waste (HLLW) is important since some of the lanthanides exhibit large neutron-capture cross-sections, hence the decreased transmutation efficiency of MA in the partitioning and transmutation strategy [1]. Currently, several two-step partitioning processes based on liquid-liquid extraction were designed: Firstly, MA(III) and Ln(III) are extracted from HLLW using oxygen-donor ligands such as CMPO [2], DMDOHEMA [3], TRPO [4] and DIDPA [5]; Next, Am(III) and Cm(III) are selectively separated from Ln(III). However, the second step, MA(III)-Ln(III)-separation, is an exceptionally challenging task owing to their similar oxidation states, chemical properties, ionic radii, and their disadvantageous ratio of presence in HLLW [6]. This separation is not feasible using common oxygen-donor ligands, but soft nitrogen- or sulphur-donor ligands can achieve sufficient selectivity for MA(III) [7]. Among a variety of nitrogen and sulphur donor extracting agents developed, 2,6-bis(5,6-dialkyl-1,2,4-trizain-3-yl)pyridines (known as BTPs) turn out to be able to perform this difficult separation from highly acidic solutions ($HNO_3 > 1$ mol/dm$^3$) with good selectivity for MA(III) over Ln(III) [8]. Furthermore, BTPs follow the carbon-hydrogen-oxygen-nitrogen (CHON) principle, i.e., BTPs consist entirely of C, H, O, and N atoms, which makes them fully combustible to safe gaseous products, minimizing the generation of secondary waste [9].

A potential process application for actual MA(III) partitioning requires that extracting agent should be chemically stable, highly soluble in organic diluent, high selectivity towards MA(III), fast kinetics and high loading capacity [9]. However, so far the available BTPs suffer from one or more drawbacks in liquid-liquid extraction system [10]. This might result in forming a third phase, multi-stage extraction procedures and disposal of large volumes of organic wastes, which requires further optimization to comply with process constrains [10]. Therefore, a series of BTP derivatives where C-H bonds in the $\alpha$-positions of the triazinyl rings are replaced by C-C bonds have been developed to improve the properties of extracting agents [7, 9, 10]. On the other hand, these problems can be alleviated by the use of alternative methods such as extraction chromatography [11–14]. Compared to liquid-liquid extraction method, the advantages of the MA(III) partitioning process based on extraction chromatography are the total insolubility of adsorbent in aqueous phase, China Academy of Engineering Physics, physical degradation, reduced radioactive waste inventory, compact equipment and no disposal of toxic organic solvents as waste [15]. Furthermore, compared to U and Pu, the minor actinides are significantly less abundant in the spent fuel, so the scale of the separation process for minor actinides from HLLW should be considerably smaller than that of the PUREX process [16].

To avoid the drawbacks of the liquid-liquid extraction process using BTPs as extracting agent and take full advantage of extraction chromatography method, we have reported a direct separation process of MA(III) based on extraction chromatography, which uses a single-column packed with silica/polymer-based *iso*Hex-BTP adsorbent named as

* Supported by National Natural Science Foundation of China (Nos. 11305102, 91126006, 21261140335 and 91226111) and Doctoral Fund of Ministry of Education of China (No. 20130073110046)
† Corresponding author, yzwei@sjtu.edu.cn

*iso*Hex-BTP/$SiO_2$-P (*iso*Hex-BTP: 2,6-bis(5,6-di*iso*hexyl)-1,2,4-triazin-3-yl)pyridine) (Fig. 1) [17, 18]. The *iso*Hex-BTP/$SiO_2$-P adsorbent, using silica/polymer composite support ($SiO_2$-P) as the inert support and *iso*Hex-BTP as the extractant, was prepared. $SiO_2$-P support contains a macroreticular styrene-divinylbenzene copolymer which is immobilized in porous silica particles with pore size of 0.6 μm and mean diameter of 60 μm. The content of extracting agent *iso*Hex-BTP reached up to 33.3% of the total mass of the adsorbent, so the adsorbent may overcome the limitation of the low solubility of BTPs in traditional aliphatic diluents. The other advantages of the partitioning process include its high adsorption selectivity and adsorption capacity, a minimal organic solvent, compact equipment, and the clean separation of MA(III).

In the present work, effects were made to study the initial nitric acid concentration and contact time on the adsorption of $^{241}$Am(III) and $^{152}$Eu(III) by *iso*Hex-BTP/$SiO_2$-P, with a batch adsorption method. The adsorption kinetics, isotherm and thermodynamics of stable nuclide Eu(III) (as a representative element of Ln(III) and a simulated element of MA(III)) by *iso*Hex-BTP/$SiO_2$-P were also determined.

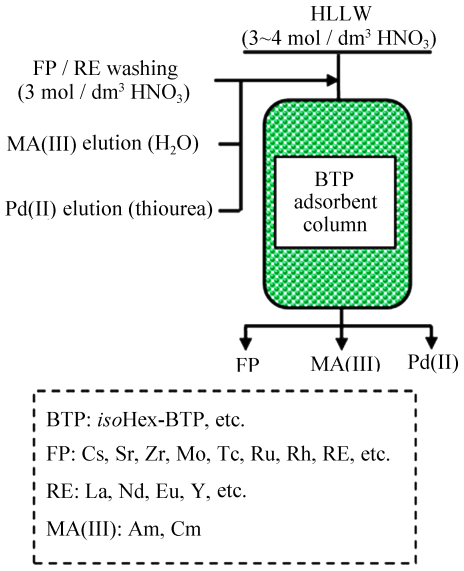


Fig. 1. (Color online) Conceptual flowchart of direct separation process of MA(III) from fission products in HLLW by extraction chromatography.

## II. EXPERIMENTAL

### A. Materials

Trace amount of $^{241}$Am(III) and $^{152}$Eu(III) (1000 Bq/cm$^3$ each) were prepared from their stocked solutions. Nitrate of Eu(III) ($Eu(NO_3)_3{\cdot}6H_2O$) reagent was of commercial reagent of analytical grade. The solutions of Eu(III) were prepared by dissolving $Eu(NO_3)_3{\cdot}6H_2O$ into nitric acid solutions.

The synthesized *iso*Hex-BTP reagent was of 99% purity. The *iso*Hex-BTP/$SiO_2$-P adsorbent was prepared as described in the previous studies of Wei *et al*. [19, 20] by impregnating *iso*Hex-BTP molecules into the pores of the silica/polymer composite support ($SiO_2$-P). *iso*Hex-BTP/$SiO_2$-P contained 0.5 g of *iso*Hex-BTP in 1.0 g of $SiO_2$-P, i.e. the content of extracting agent *iso*Hex-BTP was as high as 33.3% of the total mass of the adsorbent.

### B. Batch adsorption experiment

The adsorption of $^{241}$Am(III) and $^{152}$Eu(III) by the *iso*Hex-BTP/$SiO_2$-P adsorbent was studied in a batch adsorption mode. For each batch of experiment, 0.1 g *iso*Hex-BTP/$SiO_2$-P was taken in a glass vial with Teflon stopper. The 5-cm$^3$ solution containing $^{241}$Am(III) and $^{152}$Eu(III) (1000 Bq/cm$^3$ each) and nitric acid was added to the adsorbent. The mixture was shaken mechanically at 120 rpm for predetermined contact time at 298 K. The aqueous phase was filtrated through a membrane filter with 0.20 μm pore. The radioactivity of $^{241}$Am or $^{152}$Eu was measured by HPGe-γ-spectrometry (GEM70P-PLUS, Ortec). The distribution coefficient ($K_d$, cm$^3$/g) was calculated by Eq. (1):

$$K_d = [(A_0 - A_f)/A_f](V/W_R), \quad (1)$$

where $A_0$ and $A_f$ (in Bq/cm$^3$) are radioactivity of the radionuclides in initial and final aqueous phase, respectively; $V$ is volume of the aqueous phase (cm$^3$); and $W_R$ is weight of the *iso*Hex-BTP/$SiO_2$-P (g).

The effects of adsorption parameters including contact time (10 min–72 h), Eu(III) concentration and adsorption temperature (288 ± 1, 298 ± 1 and 308 ± 1 K) on the adsorption of stable nuclide Eu(III) by *iso*Hex-BTP/$SiO_2$-P were studied in a batch adsorption mode as described above. The concentration of Eu(III) in aqueous phase before and after adsorption was analyzed by inductively coupled plasma atomic emission spectroscopy (ICP-AES: Shimadzu ICPS-7510). The equilibrium adsorption capacity, $q_e$ (mmol/g), and the adsorption capacity at time $t$, $q_t$ (mmol/g), were obtained using Eqs. (2) and (3).

$$q_e = (C_0 - C_e)V/(1000W_R), \quad (2)$$

$$q_t = (C_0 - C_t)V/(1000W_R), \quad (3)$$

where $C_0$ (mmol/dm$^3$) and $C_e$ (mmol/dm$^3$) are Eu(III) concentration in initial aqueous phase and at equilibrium, respectively; $C_t$ (mmol/dm$^3$) is Eu(III) concentration in aqueous phase at a given contact time $t$; $V$ is volume of the aqueous phase (cm$^3$); and $W_R$ is the weight of *iso*Hex-BTP/$SiO_2$-P (g).

Most of the experiments were repeated twice for better accuracy and blank experiments were performed. The experimental error was within ±5%.

## III. RESULTS AND DISCUSSION

### A. Effect of initial nitric acid concentration on adsorption of $^{241}$Am(III) and $^{152}$Eu(III)

Figure 2 shows the distribution coefficients of $^{241}$Am(III) and $^{152}$Eu(III) towards *iso*Hex-BTP/$SiO_2$-P at nitric acid concentrations of 0.01–4 mol/dm$^3$. From Fig. 2, the separation factors between $^{241}$Am(III) and $^{152}$Eu(III) were calculated as $SF_{Am/Eu}$ = 2, 7, 28, 88, 61 and 30 at $[HNO_3]_{initial}$ = 0.01, 0.5, 1, 2, 3 and 4 mol/dm$^3$, respectively.

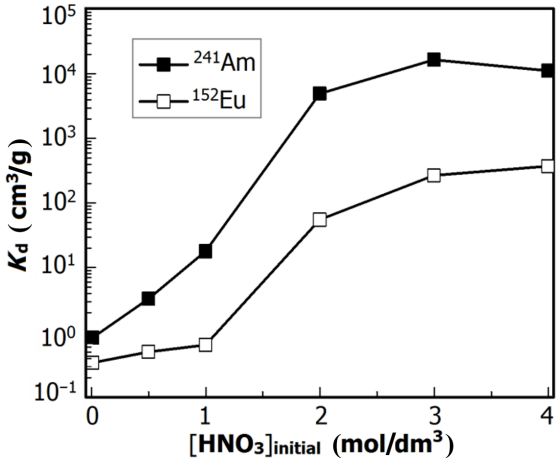


Fig. 2. Effect of initial nitric acid concentration on the distribution coefficients of $^{241}$Am(III) and $^{152}$Eu(III) by *iso*Hex-BTP/$SiO_2$-P (298 K, phase ratio: 0.1 g/5 cm$^3$, $^{241}$Am(III) and $^{152}$Eu(III): 1000 Bq/cm$^3$ each, shaking speed: 120 rpm, contact time: 24 h).

It can be seen that the distribution coefficient values of $^{241}$Am(III) increased with initial nitric acid concentration due to the consumption of nitrate in complexation reaction between Am(III) and *iso*Hex-BTP/$SiO_2$-P, and reached the maximum value ($K_d$ = 16 246 cm$^3$/g) at 3 mol/dm$^3$ nitric acid, and then decreased slightly at > 3 mol/dm$^3$ nitric acid due to the competition reaction between Am(III) and $HNO_3$ with *iso*Hex-BTP/$SiO_2$-P [8]. High distribution coefficients (> 4869 cm$^3$/g) of $^{241}$Am(III) indicated $^{241}$Am(III) quantitative adsorption from 2–4 mol/dm$^3$ nitric acid medium. Meanwhile, $^{152}$Eu(III) showed weak adsorption within the experimental nitric acid concentration range of 0.01–4 mol/dm$^3$. $SF_{Am/Eu}$ was over 60 in 2–3 mol/dm$^3$ nitric acid solutions.

From Fig. 2, the adsorbed Am(III) can be stripped into dilute nitric acid (< 0.1 mol/dm$^3$) or distilled water because Am(III) showed almost no adsorption at ≤ 1 mol/dm$^3$ nitric acid and hence adsorption of Am(III) is readily reversible by changing the nitric acid concentration.

### B. Effect of contac time on adsorption of $^{241}$Am(III) and $^{152}$Eu(III)

The distribution coefficient values of $^{241}$Am(III) and $^{152}$Eu(III) from 3 mol/dm$^3$ nitric acid as a function of contact time are presented in Fig. 3. The separation factors between $^{241}$Am(III) and $^{152}$Eu(III) calculated form Fig. 3 are $SF_{Am/Eu}$ = 55, 42, 31, 26, 56 and 74 at 0.5, 1, 3, 6, 12 and 24 h, respectively. The distribution coefficients of $^{241}$Am(III) by *iso*Hex-BTP/$SiO_2$-P increased rapidly to 6535 cm$^3$/g within the first 3 h of contact and the subsequently slow adsorption of $^{241}$Am(III) followed which continued for a relatively long period time until adsorption equilibrium was attained. The distribution coefficient of $^{241}$Am(III) reached up to 19 413 cm$^3$/g at 24 hours of contact, but the equilibrium state was not still attained. So the kinetics is considerably slow. Contrastively, $K_d$ values of $^{152}$Eu(III) were always low and below 504 cm$^3$/g within the experimental contact time range. $SF_{Am/Eu}$ was fairly high (> 50) within 30 min and over 12 hours of contact.

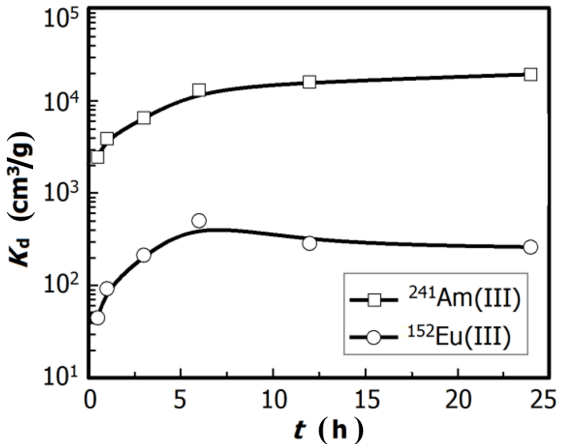


Fig. 3. Effect of contact time on the distribution coefficients of $^{241}$Am(III) and $^{152}$Eu(III) (298 K, 3 mol/dm$^3$ $HNO_3$, phase ratio: 0.1 g/5 cm$^3$, $^{241}$Am(III) and $^{152}$Eu(III): 1000 Bq/cm$^3$ each, shaking speed: 120 rpm).

From the results above, *iso*Hex-BTP/$SiO_2$-P exhibited a good selectivity and affinity for $^{241}$Am(III) over $^{152}$Eu(III) with relatively high separation factors at nitric acid concentration of 3 mol/dm$^3$ within the experimental contact time of 0.5–24 h.

Prior to the column studies, it was required to study the adsorption kinetics, isotherm and thermodynamics to design MA(III) separation system by extraction chromatography method if suitable for application. Since the adsorption behavior of Eu(III) by BTP/$SiO_2$-P adsorbent is similar to that of MA(III) owing to their similar coordination chemistry [21] and Eu(III) is a typical fission lanthanide present in HLLW, as a representative element of Ln(III) and a simulated element of MA(III), the adsorption of stable nuclide Eu(III) by *iso*Hex-BTP/$SiO_2$-P was studied to evaluate the adsorption kinetics, isotherm and thermodynamics in this work.

### C. Adsorption kinetics of Eu(III)

To obtain the information on how the amount of adsorbed Eu(III) changes with contact time and about the pro-

TABLE 1. The adsorption kinetic model parameters of Eu(III) adsorption by *iso*Hex-BTP/$SiO_2$-P at 288, 298 and 308 K

| $T$(K) | Pseudo-first-order kinetic model | | | Pseudo-second-order kinetic model | | | | Experimental |
|---|---|---|---|---|---|---|---|---|
| | $q_{e,calc}$ (mmol/g) | $k_1$ ($h^{-1}$) | $R^2$ | $q_{e,calc}$ (mmol/g) | $k_2$ (g/(mmol h)) | $h$ (mmol/(g h)) | $R^2$ | $q_{e,exp}$ (mmol/g) |
| 288 | 0.11 | 0.08 | 0.936 | 0.14 | 3.56 | 0.07 | 0.989 | 0.15 |
| 298 | 0.06 | 0.13 | 0.574 | 0.16 | 13.16 | 0.33 | 1.000 | 0.16 |
| 308 | 0.04 | 0.19 | 0.915 | 0.16 | 25.57 | 0.70 | 1.000 | 0.16 |

cess time required to achieve equilibrium between the aqueous and the adsorbent, the adsorption kinetics of Eu(III) by *iso*Hex-BTP/$SiO_2$-P was investigated. In this series of experiments, the initial concentration of Eu(III) was approximately 6 mmol/$dm^3$ and the initial nitric acid was 3 mol/$dm^3$. The adsorption capacity of Eu(III) by *iso*Hex-BTP/$SiO_2$-P against contact time at each temperature is given in Fig. 4. It was observed that the adsorption process occurred in two steps. The first step involved rapid Eu(III) uptake within the first 3 h of contact that was followed by a steady stage which finally reached an apparent plateau in 12 h at 298 K. Over 43%, 82% and 93% of the equilibrium adsorption capacity of Eu(III) occurred within the first 3 h at 288, 298 and 308 K, respectively. The sudden increase of $q_t$ at the very beginning of the process is attributed to an abundant availability of active sites on internal and external surface area of *iso*Hex-BTP/$SiO_2$-P. With the progressive occupancy of these sites by Eu(III), the process comes into a period of slower adsorption, during which the less accessible sites can be occupied by Eu(III).

The equilibrium adsorption capacity ($q_{e,exp}$) of Eu(III) was 0.15 mmol/g at 288 K and 0.16 mmol/g at 308 K (Fig. 4 and Table 1).

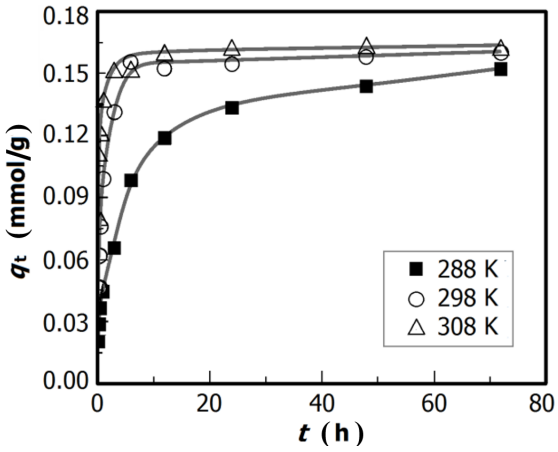


Fig. 4. Effect of contact time on adsorption capacity of Eu(III) by *iso*Hex-BTP/$SiO_2$-P at different temperatures ($[HNO_3]_{initial}$: 3 mol/$dm^3$, $[Eu(III)]_{initial}$: 6 mmol/$dm^3$, phase ratio: 0.1 g/5 $cm^3$, shaking speed: 120 rpm).

To analyzed the adsorption kinetics of Eu(IIII) by *iso*Hex-BTP/$SiO_2$-P, the pseudo-first-order and the pseudo-second-order kinetic models were applied to the experimental data.

The linear form of the pseudo-first-order kinetic model can be written as Eq. (4) [22, 23]

$$\lg(q_e - q_t) = \lg q_e - k_1 t, \tag{4}$$

where $q_e$ and $q_t$ (in mmol/g) are adsorption capacity of the metal ions at equilibrium and time ($t$), respectively; and $k_1$ ($h^{-1}$) is the adsorption rate constant.

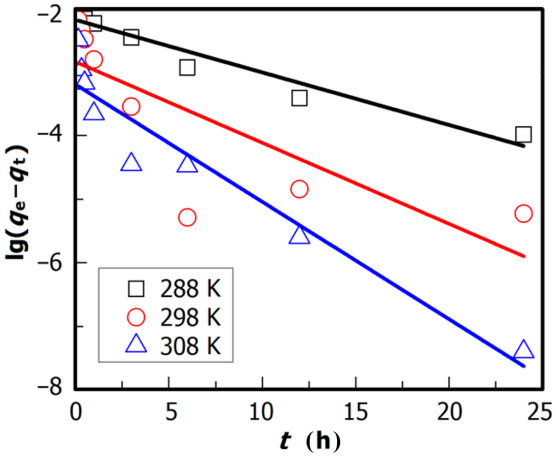


Fig. 5. (Color online) Pseudo-first-order kinetic plots of Eu(III) by *iso*Hex-BTP/$SiO_2$-P at 288, 298 and 308 K ($[HNO_3]_{initial}$: 3 mol/$dm^3$, $[Eu(III)]_{initial}$: 6 mmol/$dm^3$, phase ratio: 0.1 g/5 $cm^3$, shaking speed: 120 rpm).

The pseudo-first-order kinetic plots for Eq. (4) were made for Eu(III) adsorption by *iso*Hex-BTP/$SiO_2$-P at different temperatures (Fig. 5). The values of $k_1$, the calculated equilibrium adsorption capacity ($q_{e,calc}$) and the correlation coefficients ($R^2$) at different temperatures were calculated (Table 1). $R^2$ values for this model were fairly low ($< 0.936$), and $q_{e,calc}$ decreased with increasing temperature from 288 K to 308 K. The results conflicted with the experimental phenomena, so the experimental kinetic data could not fit to the pseudo-first-order kinetic model. The pseudo-first-order model fits experimental data well for an initial period of the first reaction step, but this model could not provide the best correlation for chemical adsorption process over long periods [23].

The experimental data were also applied to the pseudo-second-order kinetic model. The linear form of the model can be expressed as Eq. (5) [23]

$$t/q_t = 1/\left(k_2 q_e^2\right) + t/q_e, \tag{5}$$

where $q_t$ and $q_e$ (in mmol/g) are adsorption capacity of the mental ions at time $t$ and equilibrium, respectively; $k_2$ (g/(mmol h)) is the pseudo-second-order rate constant.

The kinetic data of $t/q_t$ versus $t$ for Eu(III) adsorption at different temperatures are plotted in Fig. 6. The kinetic parameters including $k_2$, the calculated equilibrium adsorption

capacity ($q_{e,calc}$), $h$ ($h = k_2 q_e^2$, initial adsorption rate) and $R^2$ (correlation coefficient) at different temperatures were calculated from the plots, as listed in Table 1.

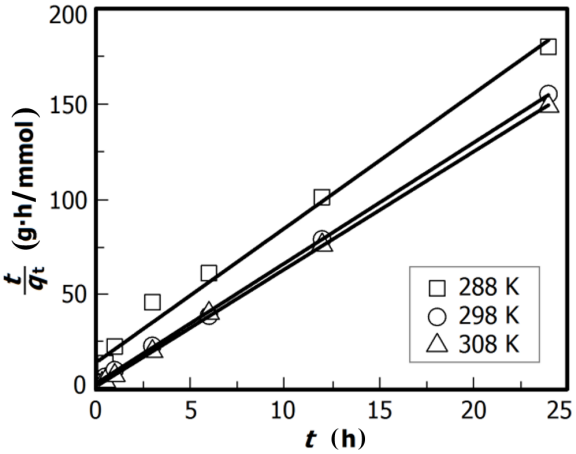


Fig. 6. Pseudo-second-order kinetic plots for the adsorption of Eu(III) by *iso*Hex-BTP/$SiO_2$-P at 288, 298 and 308 K ($[HNO_3]_{initial}$: 3 mol/dm$^3$, $[Eu(III)]_{initial}$: 6 mmol/dm$^3$, phase ratio: 0.1 g/5 cm$^3$, shaking speed: 120 rpm).

From Table 1, the correlation coefficient of the pseudo-second-order kinetic model ($> 0.989$) was much higher than that of the pseudo-first-order kinetic model ($< 0.936$) at each temperature. Since chemisorption processes show a good compliance with the pseudo-second-order kinetic model and this model is more likely to predict the kinetic behavior of adsorption with chemical reaction being the rate-controlling step [23], it can be inferred that the adsorption of Eu(III) occurred by chemisorption and the chelation reaction between Eu(III) and *iso*Hex-BTP /$SiO_2$-P is the rate-controlling step of the adsorption process [8, 23]. From 288 K to 308 K, the calculated equilibrium adsorption capacities increased slightly ($q_{e,\,calc}$ = 0.14 and 0.16 mmol/g), whereas the rate constant $k_2$ and initial adsorption rate $h$ increased dramatically from 3.56 g/(mmol h) to 25.57 g/(mmol h) and from 0.07 mmol/(g h) to 0.70 mmol/(g h), respectively. The results were consistent with the experimental phenomena. This may be due to the increase in chemisorption rate as the rate-determining step and acceleration of diffusibility of Eu(III) in solution at higher temperatures.

### D. Adsorption isotherms of Eu(III)

The adsorption capacity of Eu(III) is determined as a function of Eu(III) concentration at a constant temperature that could be explained in adsorption isotherms. The adsorption isotherm of Eu(III) by *iso*Hex-BTP/$SiO_2$-P was obtained at 3 mol/dm$^3$ nitric acid, contact time of 72 h (to obtain the complete equilibrium state) by changing the initial concentration of Eu(III) within the range of 2–6 mmol/dm$^3$, as shown in Fig. 7. The adsorption capacity of Eu(III) increased with the equilibrium concentration of Eu(III) in aqueous phase at different temperatures. Since the total existing adsorption sites of *iso*Hex-BTP/$SiO_2$-P were confined, adsorption finally reached an apparent plateau and saturation adsorption at higher concentration of Eu(III). The maximum adsorption capacity ($q_{m,exp}$) of Eu(III) increased slightly by raising the temperature (Table 2).

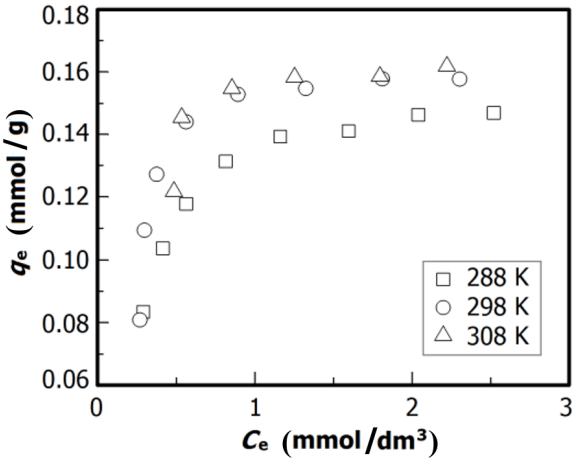


Fig. 7. Adsorption isotherms of Eu(III) by *iso*Hex-BTP/$SiO_2$-P at 288, 298 and 308 K (phase ratio: 0.1 g/5 cm$^3$, contact time: 72 h, shaking speed: 120 rpm).

The equilibrium relationship between Eu(III) concentration in the liquid phase and the concentration in *iso*Hex-BTP/$SiO_2$-P at individual temperature was analyzed by the Langmuir and Freundlich isotherm models [22].

The Freundlich equation is used to describe the adsorption of an adsorbate on a heterogeneous surface of an adsorbent. The logarithmic linear form of the model is given as Eq. (6) [23]

$$\lg q_e = \lg K_F + (\lg C_e)/n, \tag{6}$$

where $K_F$ and $n$ are the Freundlich constants which relate to the adsorption capacity and the adsorption intensity, respectively. The plots of $\lg q_e$ vs. $\lg C_e$ for Eu(III) adsorption by *iso*Hex-BTP/$SiO_2$-P are depicted in Fig. 8. The $n$ and $K_F$ constants calculated from the slop and intercept of the lines at different temperatures are listed in Table 2.

The Langmuir model which is widely used for modeling adsorption data at equilibrium is valid for monolayer adsorption on a surface. Mathematically, the model may be represented in the linear form given in Eq. (7) [23]

$$C_e/q_e = 1/(K_L q_m) + C_e/q_m, \tag{7}$$

where $q_e$ (mmol/g) is the equilibrium amount of an adsorbate adsorbed per specific amount of adsorbent, $C_e$ (mmol/dm$^3$) is the equilibrium concentration of an adsorbate in solution, $q_m$ (mmol/g) is the maximum adsorption capacity of metal ions required to form a monolayer onto an adsorbent surface, and $K_L$ (dm$^3$/mmol) is Langmuir adsorption constant related to the adsorption affinity.

TABLE 2. Equilibrium parameters evaluated at 288, 298 and 308 K by applying the Freundlich and Langmuir adsorption isotherm models to the adsorption data

| $T$(K) | Freundlich isotherm parameters | | | Langmiur isotherm parameters | | | | Experimental |
|---|---|---|---|---|---|---|---|---|
| | $n_F$ | $K_F$ (mmol/g) | $R^2$ | $q_{m,calc}$ (mmol/g) | $K_L$ (dm$^3$/mmol) | $R_L$ | $R^2$ | $q_{m,exp}$ (mmol/g) |
| 288 | 4.14 | 0.13 | 0.850 | 0.16 | 4.50 | 0.10–0.04 | 0.998 | 0.15 |
| 298 | 4.22 | 0.14 | 0.638 | 0.17 | 5.89 | 0.08–0.03 | 0.992 | 0.16 |
| 308 | 7.28 | 0.15 | 0.566 | 0.17 | 7.73 | 0.07–0.02 | 0.996 | 0.16 |

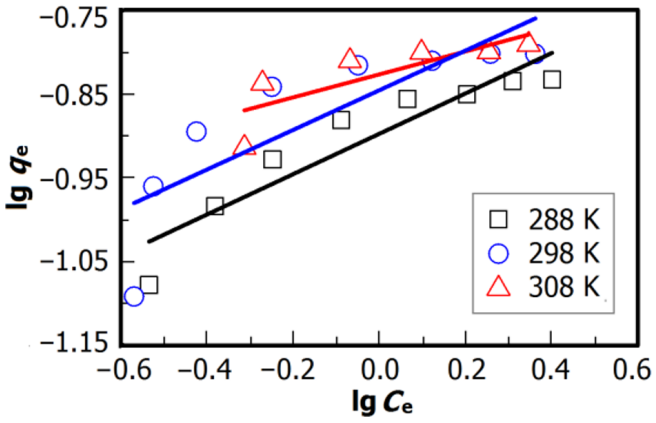


Fig. 8. (Color online) Freundlich isotherm plots for Eu(III) adsorption by *iso*Hex-BTP/$SiO_2$-P at 288, 298 and 308 K ($[HNO_3]_{initial}$: 3 mol/dm$^3$, phase ratio: 0.1 g/5 cm$^3$, contact time: 72 h, shaking speed: 120 rpm).

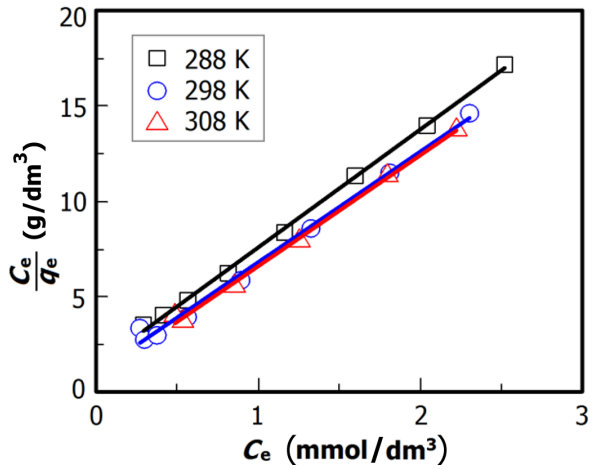


Fig. 9. (Color online) Langmuir isotherm plots for the adsorption of Eu(III) by *iso*Hex-BTP/$SiO_2$-P at 288, 298 and 308 K ($[HNO_3]_{initial}$: 3 mol/dm$^3$, phase ratio: 0.1 g/5 cm$^3$, contact time: 72 h, shaking speed:120 rpm).

The fundamental characteristic of a Langmuir isotherm parameter ($R_L$) can be expressed in terms of a dimensionless separation factor or an equilibrium parameter, which is defined by the following equation [22]:

$$R_L = 1/(1 + K_L C_0), \tag{8}$$

where $C_0$ (mmol/dm$^3$) is the initial concentration of an adsorbate. According to the value of $R_L$, the isotherm shape may be interpreted as follows:

- $R_L > 1$: unfavorable adsorption,
- $R_L = 1$: linear adsorption,
- $0 < R_L < 1$: favorable adsorption,
- $R_L = 0$: irreversible adsorption [22].

A plot of $C_e/q_e$ versus $C_e$ would result in a straight line with a slope $(1/q_m)$ and interpret of $(1/K_L q_m)$ as given in Fig. 9. Langmuir parameters for fitting adsorption data at various temperatures are listed in Table 2. The adsorption data was much better described with the Langmuir isotherm model ($R^2 \geq 0.992$) over the whole concentration range at various temperatures compared to the Freundlich isotherm model ($R^2 \leq 0.850$) based on the correlation coefficient values. The better fit to the Langmuir model can be explained the monolayer adsorption of Eu(III) by *iso*Hex-BTP/$SiO_2$-P and each adsorptive site can be occupied only once in a one-on-one manner [22]. The maximum adsorption capacity ($q_{m,calc}$ and $q_{m,exp}$) increase slightly with temperature. This may be attributed to the utilization of all available active sites for adsorption at higher temperatures. The adsorption constant $K_L$ increased by raising the temperature, indicating the adsorption affinity increasing. The value of $R_L$ ($0 < R_L < 1$) reveals that the adsorption of Eu(III) by *iso*Hex-BTP/$SiO_2$-P is favorable.

### E. Adsorption thermodynamics of Eu(III)

In order to explain the increase in adsorption with temperature (as described in the results of adsorption kinetics and isotherms), the thermodynamic parameters, i.e. change in enthalpy ($\Delta H$), entropy ($\Delta S$) and Gibbs free energy ($\Delta G$) associated to the adsorption process were determined using the following equations [23, 24]:

$$\ln K_d = \Delta S/R - \Delta H/(RT), \tag{9}$$

$$\Delta G = \Delta H - T\Delta S, \tag{10}$$

where $K_d$ is the distribution coefficient, $T$ (K) is temperature and $R$ (8.13 J/(mol K)) is the universal gas constant.

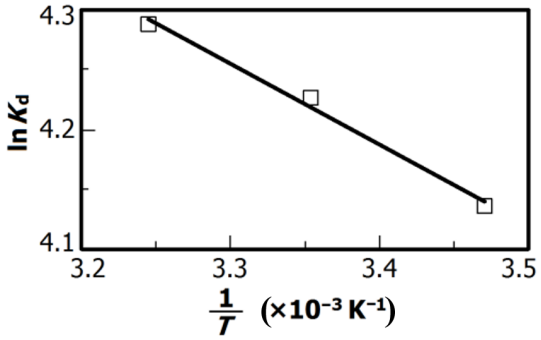


Fig. 10. The plot of $\ln K_\mathrm{d}$ versus $1/T$ for the Eu(III) adsorption by *iso*Hex-BTP/$SiO_2$-P ($[HNO_3]_{initial}$: 3 mol/dm$^3$, $[Eu(III)]_{initial}$: 5.5 mmol/dm$^3$, phase ratio: 0.1 g/5 cm$^3$, shaking speed: 120 rpm, contact time: 72 hours).

Figure 10 shows the relationship between $1/T$ and $\ln K_\mathrm{d}$. The calculated values are $\Delta H = 5621$ J/mol; $\Delta S = 54$ J/(mol K); and $\Delta G = -9931$, $-10\,471$ and $-11\,011$ J/mol at 288, 298 and 308 K, respectively. The negative $\Delta G$ value indicates that the process is spontaneous and feasible with high preference for Eu(III) by *iso*Hex-BTP/$SiO_2$-P. The increase in negative value of $\Delta G$ from $-9931$ J/mol at 288 K to $-11\,011$ J/mol at 308 K implies that adsorption tendency of Eu(III) by *iso*Hex-BTP/$SiO_2$-P increased as expected at higher temperatures. $\Delta H$ was positive, showing that the adsorption is endothermic, and heat was consumed to transfer Eu(III) from aqueous phase onto *iso*Hex-BTP/$SiO_2$-P and coordinate between Eu(III) and *iso*Hex-BTP/$SiO_2$-P. The positive value of $\Delta S$ suggests the increase in the degree of randomness at the solid-solution interface mostly encountered in Eu(III) binding due to the release of water molecules of the hydration sphere during the fixation of Eu(III) on *iso*Hex-BTP/$SiO_2$-P surface [22, 25]. Furthermore, positive $\Delta S$ value indicates that the adsorption process is probably irreversible and favored complexation adsorption. Although $\Delta H$ value was positive, $\Delta G$ value at each temperature was negative, indicating that the contribution of entropic term makes the free adsorption energy negative.

These results were in agreement with the results obtained from the pseudo-second-order kinetic model and Langmuir isotherm model.

## IV. CONCLUSION

In this study, batch adsorption experiments showed that *iso*Hex-BTP/$SiO_2$-P exhibited remarkable selectivity towards $^{241}$Am(III) compared to $^{152}$Eu(III) at nitric acid concentration of 2–4 mol/dm$^3$. Within the experimental contact time range of 0.5–24 h, *iso*Hex-BTP/$SiO_2$-P showed the relatively high selectivity for $^{241}$Am(III) over $^{152}$Eu(III) in 3 mol/dm$^3$ nitric acid. Various factors such as contact time, Eu(III) concentration and temperature had impacts on adsorption of stable nuclide Eu(III) (as a representative element of Ln(III) and a simulated element of MA(III)) by *iso*Hex-BTP/$SiO_2$-P. The obtained adsorption data depending on contact time provided much better fitting for the pseudo-second-order kinetic equation with high correlation coefficient ($R^2 \geq 0.989$) than the pseudo-first-order kinetic model, indicating that Eu(III) adsorption by *iso*Hex-BTP/$SiO_2$-P occurred by chemisorption mechanism as a rate-controlling step in the adsorption process. However, the adsorption kinetics of Am(III) and Eu(III) by *iso*Hex-BTP/$SiO_2$-P is slow. Furthermore, the equilibrium adsorption capacity initial adsorption rate and adsorption rate constant increased with temperature from 288 K to 308 K. The experimental adsorption isotherm fitted better to the Langmuir isotherm model than the Freundlich isotherm model at various temperatures. The maximum adsorption capacity of Eu(III) and the Langmuir adsorption constant $K_\mathrm{L}$ increased with temperature from 288 K to 308 K. The studies revealed that Eu(III) adsorption was spontaneous and endothermic process with an increase of entropy. It is expected that *iso*Hex-BTP/$SiO_2$-P has applicability in the separation of Am(III) from Eu(III) present in HLLW. Efforts are being made for more detailed property evaluation of *iso*Hex-BTP/$SiO_2$-P, and methods of improving the adsorption kinetics and the column separation experiments.



[1] Magnusson D, Geist A, Wilden A, Modolo G. Direct selective extraction of actinides(III) from PUREX raffinate using a mixture of CyMe4-BTBP and TODGA as 1-cycle SANEX solvent PART II: Flow-sheet design for a counter-current centrifugal contactor demonstration process. Solvent Extr Ion Exc, 2013, **31**: 1–11. DOI: 10.1007/BF01885923

[2] Antony M P, Kumaresan R, Suneesh A S, *et al*. Development of a CMPO based extraction process for partitioning of minor actinides and demonstration with geneuine fast reactor fuel solution (155 GWd/Te). Radiochim Acta, 2011, **99**: 207–215. DOI: 10.1007/BF01885923

[3] Patil A B, Shinde V S, Pathak P N, *et al*. Modified synthesis scheme for N,N'-dimethyl-N,N'-dioctyl-2,(2'-hexyloxyethyl) malonamide (DMDOHEMA) and its comparison with proposed solvents for actinide partitioning. Radiochim Acta, 2013, **101**: 93–100. DOI: 10.1524/ract.2013.1998

[4] Chen J and Wang J C. Overview of 30 years research on TRPO process for actinides partitioning from high level liquid waste. Prog Chem, 2011, **23**: 1366–1371.

[5] Paiva A P and Malik P. Recent advances on the chemistry of solvent extraction applied to the reprocessing of spent nuclear fuels and radioactive wastes. J Radioanal Nucl Ch, 2004, **261**: 485–496. DOI: 10.1023/B:JRNC.0000034890.23325.b5

[6] Gorden A E V, DeVore M A, Maynard B A. Maynard B A. Coordination chemistry with f-element complexes for an improved understanding of factors that contribute to extraction selectivity. Inorg Chem, 2013, **52**: 3445–3458. DOI: 10.1021/ic300887p

[7] Geist A, Hill C, Modolo G, *et al*. 6,6'-bis (5,5,8,8-tetramethyl-5,6,7,8-tetrahydro-benzo [1,2,4] triazin-3-yl) [2,2'] bipyridine,

an effective extracting agent for the separation of americium(III) and curium(III) from the lanthanides. Solvent Extr Ion Exch, 2006, **24**: 463–483. DOI: 10.1080/07366290600761936

[8] Panak P J and Geist A. Complexation and extraction of trivalent actinides and lanthanides by triazinylpyridine N-donor ligands. Chem Rev, 2013, **113**: 1199–1236. DOI: 10.1021/cr3003399

[9] Retegan T, Ekberg C, Englund S, *et al*. The behaviour of organic solvents containing C5-BTBP and CyMe4-BTBP at low irradiation doses. Radiochim Acta, 2007, **95**: 637–642. DOI: 10.1524/ract.2007.95.11.637

[10] Trumm S, Geist A, Panak P J, *et al*. An improved hydrolytically-stable Bis-Triazinyl-Pyridine (BTP) for selective actinide extraction. Solvent Extr Ion Exc, 2011, **29**: 213–229. DOI: 10.1080/07366299.2011.539129

[11] Bhattacharyya A, Mohapatra P K, Manchanda V K. Solvent extraction and extraction chromatographic separation of Am3+ and Eu3+ from nitrate medium using Cyanex® 301. Solvent Extr Ion Exc, 2007, **25**: 27–39. DOI: 10.1080/07366290601067713

[12] Liu R Q, Wang X P, Wei Y Z, *et al*. Evaluation study on a macroporous silica-based isohexyl-BTP adsorbent for minor actinides separation from nitric acid medium. Radiochim Acta, 2014, **102**: 93–100. DOI: 10.1515/ract-2014-2097

[13] Matsumura T, Matsumura K, Morita Y, *et al*. Separation of trivalent minor actinides from fission products using single R-BTP column extraction chromatography. J Nucl Sci Technol, 2011, **48**: 855–858. DOI: 10.1080/18811248.2011.9711769

[14] Liu R Q, Wei Y Z, Tozawa D, *et al*. Evaluation study on properties of a macroporous silica-based CMPO extraction resin to be used for minor actinides separation from high level liquid waste. Nucl Sci Tech, 2011, **22**: 18–24.

[15] Raju C S K and Subramanian M S. A novel solid phase extraction method for separation of actinides and lanthanides from high acidic streams. Sep Purif Technol, 2007, **55**: 16–22. DOI: 10.1016/j.seppur.2006.10.013

[16] Wei Y, Kumagai M, Takashima Y. Studies on the separation of minor actinides from high-level wastes by extraction chromatography using novel silica-based extraction resins. Nucl Technol, 2000, **132**: 413–423.

[17] Usuda S, Wei Y, Xu Y, *et al*. Development of a simplified separation process of trivalent minor actinides from fission products using novel R-BTP/SiO2-P adsorbents. J Nucl Sci Technol, 2012, **49**: 334–342. DOI: 10.1080/00223131.2012.660018

[18] Liu R Q, Wei Y Z, Xu Y L, *et al*. Evaluation study on properties of isohexyl-BTP/SiO2-P resin for direct separation of trivalent minor actinides from HLLW. J Radioanal Nucl Chem, 2012, **292**: 537–544. DOI: 10.1007/s10967-012-1631-3

[19] Wei Y Z, Hoshi H, Kumagai M, *et al*. Separation of Am(III) and Cm(III) from trivalent lanthanides by 2,6-bistriazinylpyridine extraction chromatography for radioactive waste management. J Alloy Compd, 2004, **374**: 447–450. DOI: 10.1016/j.jallcom.2003.11.059

[20] Wei Y Z, Sabharwal K N, Kumagai M, *et al*. Preparation of novel silica-based nitrogen donor extraction resins and their adsorption performance for trivalent americium and lanthanides. J Nucl Sci Technol, 2000, **37**: 1108–1110. DOI: 10.1080/18811248.2000.9714999

[21] Denecke M A, Rossberg A, Panak P J, *et al*. Characterization and comparison of Cm(III) and Eu(III) complexed with 2,6-di(5,6-dipropyl-1,2,4-triazin-3-yl)pyridine using EXAFS, TRFLS, and quantum-chemical methods. Inorg Chem, 2005, **44**: 8418–8425. DOI: 10.1021/ic0511726

[22] Javadian H, Ghaemy M, Taghavi M. Adsorption kinetics, isotherm, and thermodynamics of Hg2+ to polyaniline/hexagonal mesoporous silica nanocomposite in water/wastewater. J Mater Sci, 2014, **49**: 232–242. DOI: 10.1007/s10853-013-7697-7

[23] Dikici H, Saltali K, Bingolbali S. Equilibrium and kinetics characteristics of copper (II) sorption onto gyttja. Bull Environ Contam Tox, 2010, **84**: 147–151. DOI: 10.1007/s00128-009-9899-x

[24] Ozeroglu C and Metin N. Adsorption of uranium ions by crosslinked polyester resin functionalized with acrylic acid from aqueous solutions. J Radioanal Nucl Chem, 2012, **292**: 923–935. DOI: 10.1007/s10967-011-1533-9

[25] Salam M A. Removal of heavy metal ions from aqueous solutions with multi-walled carbon nanotubes: Kinetic and thermodynamic studies. Int J Environ Sci Te, 2013, **10**: 677–688. DOI: 10.1007/s13762-012-0127-6